

## **ALTERNARIA ALTERNATA MEDIATED SYNTHESIS OF PROTEIN CAPPED SILVER NANOPARTICLES AND THEIR GENOTOXIC ACTIVITY**

JOY SARKAR<sup>a</sup>, DIPANKAR CHATTOPADHYAY<sup>b</sup>, SRIMANTA PATRA<sup>c</sup>, SIDDHARTHA SINGH DEO<sup>a</sup>, SONALI SINHA<sup>d</sup>, MANOSIJ GHOSH<sup>d</sup>, ANITA MUKHERJEE<sup>d</sup>, KRISHNENDU ACHARYA<sup>a\*</sup>

<sup>a</sup>*Molecular and Applied Mycology and Plant Pathology Laboratory, Department of Botany, University of Calcutta, Kolkata-700019*

<sup>b</sup>*Department of Polymer Science & Technology, University College of Science & Technology, University of Calcutta, Kolkata-700009*

<sup>c</sup>*Govt. College of Engineering and Ceramic Technology, 73 A.C. Banerjee Lane, Kolkata-700010*

<sup>d</sup>*Cell Biology & Genetic Toxicology Laboratory, Centre of Advanced Study in Cell & Chromosome Research, Department of Botany, University of Calcutta, Kolkata-700009*

### **Abstract**

In recent years, rapid technological advancements have led to the development of nanoscale device components, advanced sensors, and novel biomimetic materials. Potential negative impacts of nanomaterials are sometimes overlooked during the discovery phase of research. The use of green chemistry can however enhance nanoscience by maximizing safety and efficiency while minimizing the environmental and societal impacts of nanomaterials. Here we report extracellular mycosynthesis of silver nanoparticles by *Alternaria alternata*. The fungal biomass when exposed to aqueous silver nitrate solution leads to the formation of silver nanoparticles extracellularly. Change in colour of silver nitrate solution to brown signifies the development of silver nanoparticles. UV–Visible spectrum of the aqueous medium containing silver ion showed a peak at 420 nm corresponding to the plasmon absorbance of silver nanoparticles. Agglomeration status was confirmed by Dynamic Light Scattering experiments. Atomic Force Microscopy and Transmission Electron Microscopy explained the formation of well-dispersed silver nanoparticles in the range of 20-45 nm. X-ray Diffraction spectrum of the silver nanoparticles exhibited 2θ values corresponding to the silver nanoparticles. Fourier Transform Infrared Spectroscopy confirmed the presence of a protein shell outside the nanoparticles. In this study, mycosynthesized nanoparticles were also evaluated for DNA damaging potential in human lymphocytes using comet assay.

(Received February 15, 2011; accepted March 10, 2011)

Keywords: *Ag nanoparticles, comet assay, DNA damage, Mycosynthesis.*

### **1. Introduction**

Nanotechnology is foreseen to significantly influence science, economy and everyday life in the 21<sup>st</sup> century and also to become one of the driving forces of the next industrial revolution. There is an enormous interest in the synthesis of nanomaterials due to their unusual optical [1], chemical [2], photoelectrochemical [3], and electronic [4] properties.

---

\*Corresponding author: *krish\_paper@yahoo.com*

The traditional, wet-chemical procedure is the most widely used method for synthesis of metallic nanoparticles. Chemical synthesis is cost effective; however, their drawbacks include contamination from precursor chemicals, use of toxic solvents, and generation of hazardous by-products. This has led to a growing awareness of the need to develop clean, nontoxic and environment friendly procedures for synthesis and assembly of nanoparticles. Among the biological systems, fungi have been found to be the most suitable for the synthesis of metal nanoparticles. They are easy to cultivate, reliable, ecofriendly and the methodology for extracellular synthesis is extremely cost-effective and less time consuming.

Biological systems have been widely utilized to synthesize and assemble a range of inorganic nanomaterial from bacteria [5], algae [6] and fungi [7]. Among the different microbes used for the synthesis of nanoparticles, fungi are efficient candidates for fabrication of metal nanoparticles both intra and extracellularly. The nanoparticles synthesized using fungi possess good polydispersity, dimensions and stability. Literature survey showed a number of fungi to produce nanoparticles either intracellularly or extracellularly [8, 9, 10].

Filamentous fungi in general possess some distinctive advantage over bacteria and algae, because of their high metal tolerance and bioaccumulation ability [11]. Another advantage of using fungi in nanoparticle synthesis is the ease in their scale-up. Though the fungi are extremely efficient secretors of extracellular enzymes, it is thus possible to easily obtain large-scale production of enzymes.

Silver nanoparticles find diverse applications in the field of bio labelling [12], sensors, drug delivery system [13], polarizing filters [14], electrical batteries, staining pigments and also as an antibiotic agent [15, 16]. Silver nanoparticles are known for their antibacterial properties and potent inducers of apoptosis and inflammation considering the phenotypical changes in the liver as compared to silver bulk material [17]. Several studies have demonstrated that silver nanoparticle were cytotoxic [18] and could trigger oxidative stress [17].

Despite the rapidly growing market of silver nanoparticle based products, there is still a lack of information regarding the impact on environment and human health of silver nanoparticles as well as reliable data on risk assessment [19].

The present study has two fold objectives: firstly extracellular synthesis and characterization of silver nanoparticles using a phytopathogenic fungus *Alternaria alternata* (Strain Number: MAMP/C/51) and secondly, to find the genotoxic response of silver nanoparticles in human lymphocyte using the comet assay.

## **2. Experimental**

### **2.1 Pathogen isolation and production of fungal biomass**

The infected leaves of *Rauvolfia serpentina* were brought to the laboratory and from the infected lesions, pathogen were isolated on Potato Dextrose Agar (HiMedia Laboratories Pvt. Ltd., Mumbai, India) slants following Davies' method [20]. The pathogen, *Alternaria alternata* (Strain Number: MAMP/C/51) was characterized and identified according to the monograph of Subramaniam (1971) [21], Ellis (1971, 1976) [22, 23]. The fungus was grown aerobically in liquid potato dextrose broth (HiMedia Laboratories Pvt. Ltd., Mumbai, India) medium. The Erlenmeyer flasks of capacity 250 ml was inoculated with fungal mycelia and incubated at  $30 \pm 2^\circ\text{C}$  for 10-15 days till circular fungal mat was obtained. The full-grown fungal biomass was removed and washed thoroughly with deionised water (three times). 10 g of that full-grown fungal biomass was taken in a sterilized Erlenmeyer flask which was further used for the reduction of the silver nitrate aqueous solution.

## 2.2 Synthesis of silver nanoparticles

The chemical silver nitrate ( $\text{AgNO}_3$ ) was purchased from Sigma, St. Louis, MO, USA. 100 ml of 1mM  $\text{AgNO}_3$  solution was added to the fungal biomass. The flask was incubated at 37°C in dark in a rotary shaker at 150 rpm at room temperature. Both, positive (fungal biomass with deionised water) and negative control (silver nitrate solution only) were maintained under similar conditions.

The silver nanoparticles were separated out by centrifugation (at 12000 g for 10 min), and the settled nanoparticles were washed in deionized water (three times). The purified silver nanoparticles were resuspended in deionized water and ultrasonicated by Piezo-u-sonic ultrasonic cleaner (Pus-60w) and kept at room temperature (37 °C).

## 2.3 UV-visible spectroscopic analysis of silver nanoparticles

The absorption at 420 nm (maximum absorbance observed in the full range scan) was measured continuously to determine the stability of the solution. The UV-visible spectra of the solution were recorded in a Hitachi 330 Spectrophotometer from 250 to 850 nm. Deionised water was used as blank.

## 2.4 Measuring the size by Dynamic Light Scattering Test

Particle Size was measured by laser diffractometry using a Nano Size Particle Analyzer (Zen 1600 Malvern, USA) in the range between 0.6 nm and 6.0  $\mu\text{m}$ , under the following conditions: particle refractive index 1.590, particle absorption coefficient 0.01, water refractive index 1.33, and temperature- 25°C. Fifteen measurement cycles of 10 s each were taken and the data obtained were averaged by software (DTS, Ver. 5.00 from Malvern).

## 2.5 Atomic Force Microscopic observation of silver nanoparticles

Size and the surface topography of the drop coated film of the silver nanoparticles was investigated with atomic force microscope (AFM) (Nanoscope IIIa Veeco multimode, USA) and high resolution surface images were produced. In AFM characterization, the contact mode (NP10) with a silicon probe over scan sizes of 1.96  $\mu\text{m}$  was used.

## 2.6 Transmission Electron Microscopic (TEM) observation of silver nanoparticles

TEM samples of the aqueous suspension of silver nanoparticles were prepared by placing a drop of the suspension on carbon-coated copper grids and allowing the water to evaporate. The micrographs were obtained by Tecnai G<sup>2</sup> spirit Biotwin (FP 5018/40) TEM, operated at 80 kV accelerating voltage.

## 2.7 Fourier Transform Infrared Spectroscopic (FTIR) analysis

For fourier transform infrared spectroscopic (FTIR) analysis, the vacuum dried silver nanoparticles were mixed with Potassium Bromide (KBr) at a ratio of 1:100 and the spectra were recorded with a Shimadzu 8400S fourier transform infrared spectrophotometer using a diffuse reflectance accessory. The scanning data were obtained from the average of 50 scans in between 4000 to 400  $\text{cm}^{-1}$  range. For comparison, only dried fungal biomass of *Alternaria alternata* was mixed with KBr powder and pelletized after drying properly.

## 2.8 X-ray Diffraction (XRD) measurement of silver nanoparticles

The liquid reaction mixture after bio-reduction was dried at 45°C in a vacuum drying oven. Then the dried mixture was collected for determining the formation of silver nanoparticles. The vacuum dried silver nanoparticles were used for powder X-ray diffraction (XRD) analysis.

The spectra were recorded in a PW. 3040/60 PANalytical X-ray diffractometer (Cu K $\alpha$  radiation,  $\lambda$  1.54443) running at 45 kV and 30 mA. The diffracted intensities were recorded from 2° to 99° 2 $\theta$  angles.

### **2.9 Isolation of mononuclear cells from blood**

The lymphocytes were obtained by centrifuging blood from healthy volunteers overlaid on Histopaque (Sigma Chemical Co.) according to Boyum (1976) [24] in the ratio 1:2. The lymphocytes were isolated from the interface and washed in PBS and centrifuged. The cells were resuspended in PBS for further use. All experiments were conducted in accordance with the University of Calcutta ethical guidelines.

### **2.10 Viability**

All viabilities were measured by trypan blue exclusion to avoid artefacts due to toxicity [25]. The cut-off point suggested by Henderson et al. (1997) [26] was 70%. Viability was measured both before and after treatment and range of viable cells was within 85 - 90 % in all experiments.

### **2.11 Treatment of the lymphocyte cells**

Freshly isolated human lymphocytes were incubated for 3 hours at 37 °C in RPMI-1640 media with different concentrations of nanosilver (control, 50, 100, 200, 300 and 400  $\mu$ g /ml). Positive control set was maintained in methyl methanesulphonate-MMS (100  $\mu$ M). Following treatment, the lymphocytes were processed for detection of possible DNA damage as assessed by the alkaline comet assay.

### **2.12 DNA damage analysis using Comet assay**

The DNA damage studies were carried out following the Comet assay or (SCGE) according to the method of Singh et al. (1988) [27] with modifications [28, 29]. Slides were prepared in triplicates per concentration. Slides were immersed in cold lysis solution at pH 10. The lysis solution consisted of 2.5 M NaCl (Sigma-Aldrich, USA), 100 mM Na<sub>2</sub>EDTA (Sigma-Aldrich, USA), 10 mM Trizma base (Sigma-Aldrich, USA), 1% Triton X-100 (Merck, India), 10% DMSO (Sigma-Aldrich, USA) and kept at 4 °C for 60 min. After lysis the DNA was allowed to unwind in the electrophoresis buffer [300 mM NaOH (SRL Chemicals, Mumbai, India): 1mM Na<sub>2</sub>EDTA (pH 13.5)] for 20 min. This was followed by electrophoresis conducted at a constant voltage of 25 V at 4 °C. Slides were neutralized in 0.4 M Tris (pH 7.5) for 5 min and finally rinsed in water. Each experiment was repeated twice.

The slides were then stained with 50-75 $\mu$ l of ethidium bromide (Sigma-Aldrich, USA; 20 $\mu$ g/ml) for five minutes and then rinsed in chilled water to wash off excess stain and analysed. Slides were scored using image analysis system (Kinetic imaging; Andor Technology, Nottingham, UK) attached to a fluorescence microscope (Leica, Wetzlar, Germany) equipped with appropriate filters (N2.1). The microscope was connected to a computer through a charge-coupled device (CCD) camera to transport images to software (Komet 5.5) for analysis. The final magnification was 100 X. The median values of each parameters - tail DNA (%) and the Olive tail moment (arbitrary units), were scored from each slide and expressed as means for each treatment group. Images of 150 (50  $\times$  3) cells per concentration were analysed.

### **2.13 Statistical analysis**

For statistical analysis median values of each concentration with respect to the comet parameters were calculated and one way analysis of variance (ANOVA) test was done by using

Sigma Stats. 3 software (SPSS Inc., Chicago, Illinois, USA). For all statistical analysis the level of significance was established at  $P \leq 0.05$ .

### 3. Results and discussion

#### 3.1 Production and characterization of silver nanoparticles

The fungal biomass after addition of aqueous  $\text{AgNO}_3$  (1 mM) showed a distinct change in colour of the solution within 24 hours as because the  $\text{Ag}^+$  ions gets converted to  $\text{Ag}^0$  state and the colour of the medium turns to dark brown due to reductase activity of that fungus [15]. Both the positive as well as negative control showed no significant colour change in the same experimental conditions. The reduction of silver was subjected to spectral analysis by using the UV-Vis spectrophotometer. This showed an absorbance peak at 420 nm (Fig.1), which was specific for silver nanoparticles. It might arise from the excitation of a longitudinal plasmon vibration in silver nanoparticles in the solution [30].

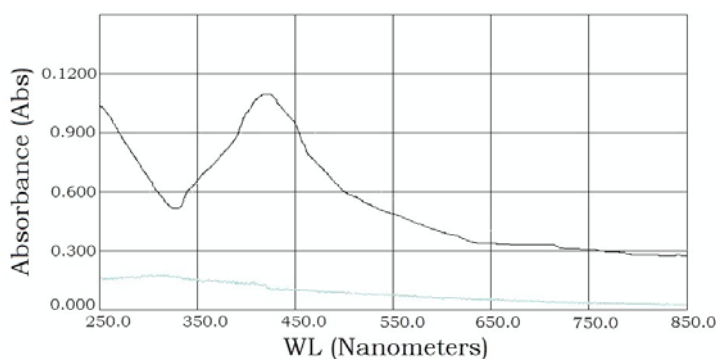


*Fig. 1 UV visible absorption spectra recorded as a function of time of reaction at  $10^{-3}$  M aqueous solution of silver nitrate with fungal biomass. The silver nanoparticle formation was monitored through UV-Visible absorption spectroscopy (excitation band near 420 nm for silver) correspond to 0 and 24 hours after incubation.*

Particle size was determined by dynamic light scattering measurement. Laser diffraction revealed the particle to be highly monodispersed, with an average diameter of  $28 \pm 4.0$  nm, in the size range of 20 to 45 nm (Fig.2). The AFM image of silver nanoparticles was shown that the nanoparticles were symmetrical and spherical in shape, monodisperse in nature and well distributed without aggregation (Fig.3). Figure 4 shown the transmission electron microscopic (TEM) image of different sizes of silver nanoparticles which arose from the bioreduction of silver nitrate solution by fungal biomass at room temperature for 24 h. These observations revealed that the homogeneous spherical silver nanoparticles formed in the reaction solution, were monodisperse in nature. The diameters of these silver nanoparticles were measured and the size was in the range of 20 to 45 nm. The average diameter of these silver nanoparticles was of  $28 \pm 4.0$  nm.

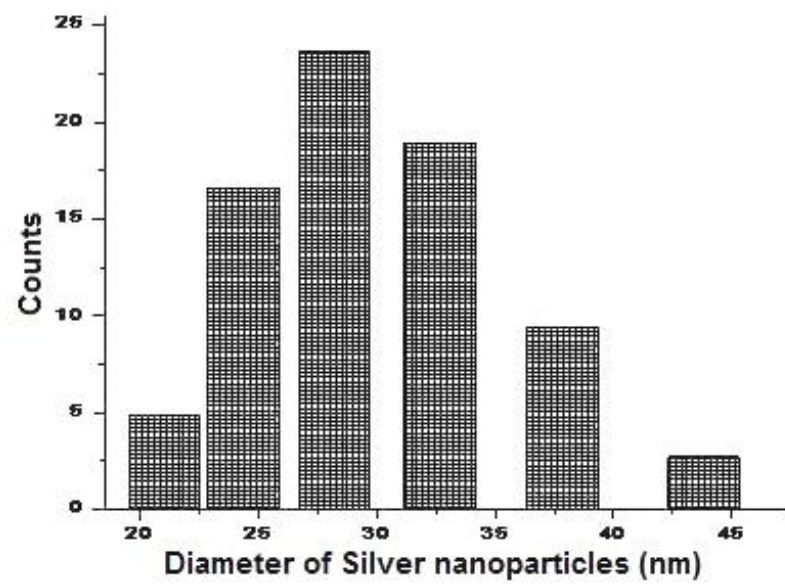


Fig. 2 Histogram of particle size distribution as obtained from light scattering of the silver nanoparticles produced by *Alternaria alternata*.

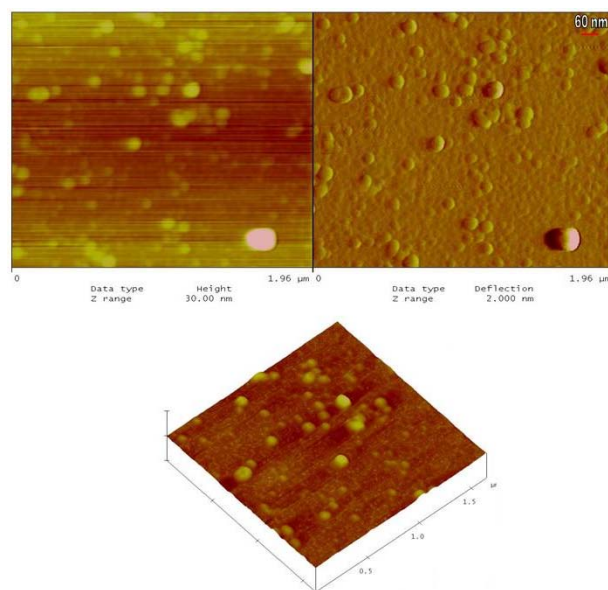
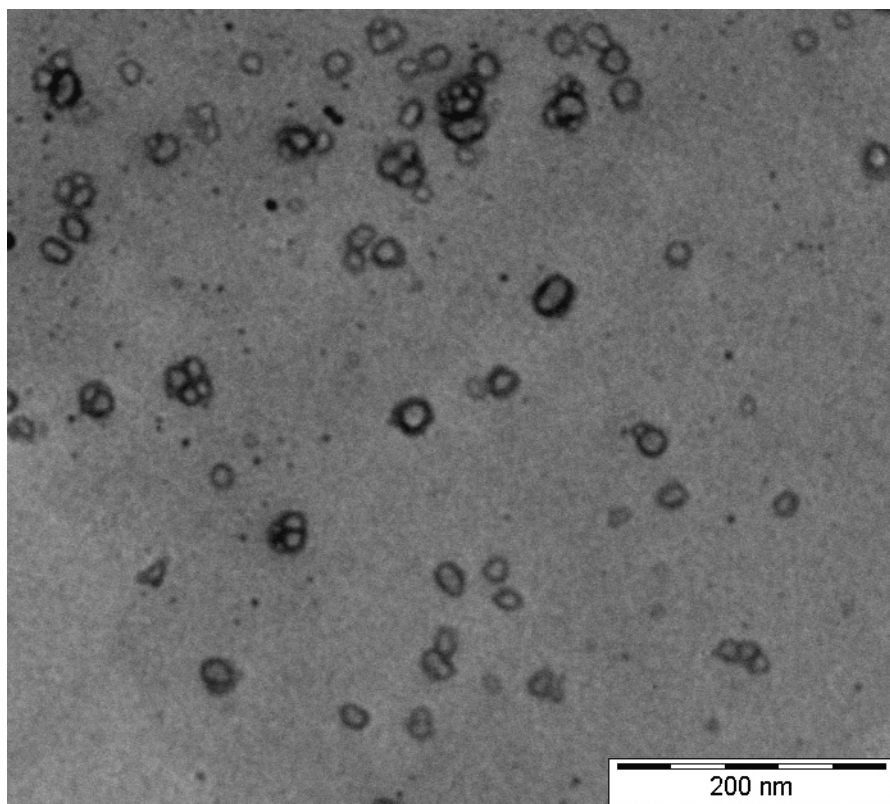


Fig. 3 AFM images of silver nanoparticles (upper) and the three dimensional view of silver nanoparticles (lower).



*Fig. 4 Transmission electron micrograph of silver nanoparticles after bio-reduction of silver nitrate.*

An earlier IR spectroscopic study confirmed that the carbonyl group of amino acid residues and peptides have a stronger ability to bind metal, and the proteins could most possibly form a coat covering the metal nanoparticles (i.e. capping of silver nanoparticles) to prevent the agglomeration of the particles [31]. Typical FTIR absorption spectra of fungal biomass before and after bio-reduction were shown in the figure 5 (a) and 5 (b) respectively. Both of them showed the presence of bonds due to O-H stretching (around  $3430\text{ cm}^{-1}$ ), aldehydic C-H stretching (around  $2910\text{ cm}^{-1}$ ), C=C group (around  $1600\text{ cm}^{-1}$ ), -COO stretching (around  $1450\text{ cm}^{-1}$ ), and -C-O-C-stretching (around  $1070\text{ cm}^{-1}$ ) [32, 33, 34, 35, 36, 37]. These peaks indicated the presence of proteins and other organic residues, which might have diffused from the mycelial mat in water under normal pH conditions (pH 7.1). Bands at around  $1650$ ,  $1550$  and  $1250\text{ cm}^{-1}$  indicated the amide linkages between the amino acid residues in proteins, which give rise to the well known signature in the infra-red regions of the electro-magnetic spectrum. The bands visible in between  $500$  to  $750\text{ cm}^{-1}$  signified the presence of R-CH group which is abundantly found in fungal cell filtrate. Infrared active modes attributed to side chain vibrations include C-H stretching symmetric and anti-symmetric modes at around  $2920$  and  $2850\text{ cm}^{-1}$  corresponding to aliphatic and aromatic modes respectively [38]. A new band visible only at  $1394\text{ cm}^{-1}$  in the figure 5 b showed the presence of  $-\text{NO}_3$  which was derived from  $\text{AgNO}_3$  [36, 37]. With the overall observations, it can be concluded that the proteins might have formed a coating over the silver nanoparticles, which in turn supports their stabilization for several months.

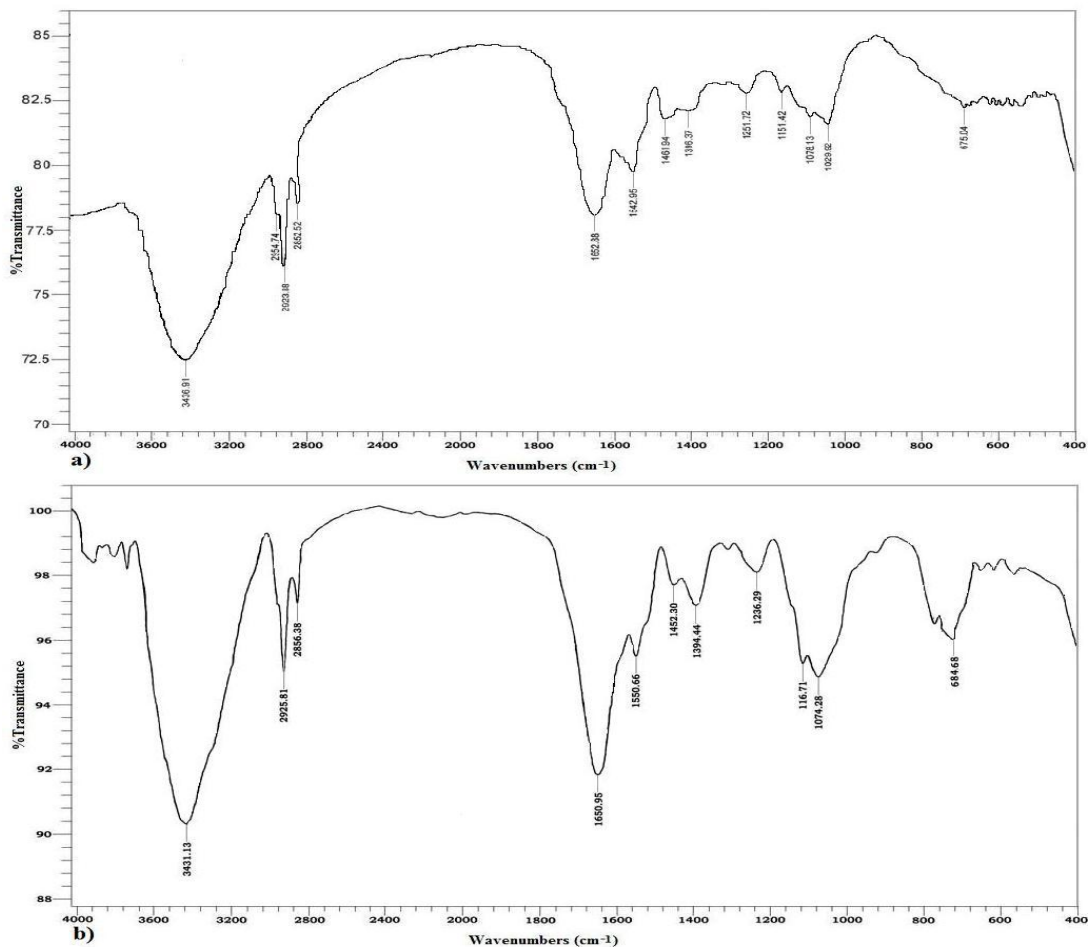


Fig. 5 FTIR absorption spectra of fungal biomass before (a) and after (b) bioreduction

The exact nature of the silver particles formed was achieved by measuring the XRD-spectrum of the samples. Inspection of the XRD patterns of vacuum dried silver nanoparticles reveals the existence of sharp diffraction lines at low angles ( $2^\circ$  to  $99^\circ$ ). The silver nanoparticles exhibited peaks of silver at  $2\theta=38^\circ$ ,  $44^\circ$ ,  $64^\circ$  and  $78^\circ$  that can be indexed to the (111), (200), (220) and (311) facets of silver, respectively (Fig.6). The XRD-spectrum measurement resulted in four intense peaks, observed spectrum agree to the Bragg's reflection of silver nano-crystals reported in literature [39]. This further confirms that silver nanoparticles formed in the extracellular filtrate are present in the form silver nano crystals.

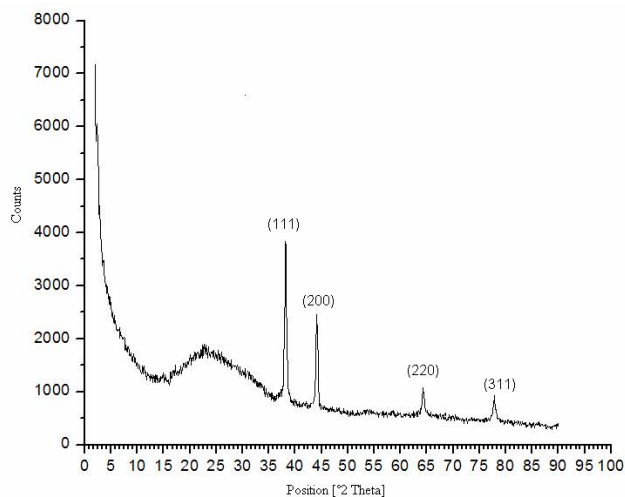


Fig. 6 X-ray diffraction pattern of silver nanoparticles.

### 3.2 Genotoxicity of silver nanoparticles

The trypan blue dye exclusion method was performed in order to evaluate cell viability after exposure of blood cells/ lymphocytes to different concentration of these silver nanoparticles. Results are expressed as percentage of the control and represent the mean of two experiments, each in triplicate. No significant change in viability occurred in the exposed cells compared with the untreated control cells (data not shown).

Following *in vitro* treatment with silver nanoparticles at different concentrations, lymphocytes were analyzed using comet assay for any probable DNA damage (Fig.7). With the increase in concentration of silver nanoparticles there was an increase in DNA damage till 300  $\mu\text{g}/\text{ml}$  as represented in terms of percentage of DNA in the Tail (% Tail DNA) and Olive Tail Moment (OTM). Responses were statistically significant at the two higher concentrations (300  $\mu\text{g}/\text{ml}$  and 400  $\mu\text{g}/\text{ml}$ ). The values of comet parameters were  $\sim 5$ -fold higher in the positive control (100  $\mu\text{M}$  MMS) as compared to the lowest treatment dose.

Genotoxicity of starch-coated silver nanoparticles in human lung fibroblast cells (IMR-90) and human glioblastoma cells (U251) was demonstrated elegantly by Asharani et al. 2009 [40]. Extensive and dose-dependent damage to DNA was observed after treatment of the cells with silver nanoparticles. Comet assay of silver nanoparticles treated cells showed a concentration dependent increase in tail moment as compared to control cells. Our results on human lymphocytes are in line with that reported by Asharani et al. 2009 [40].

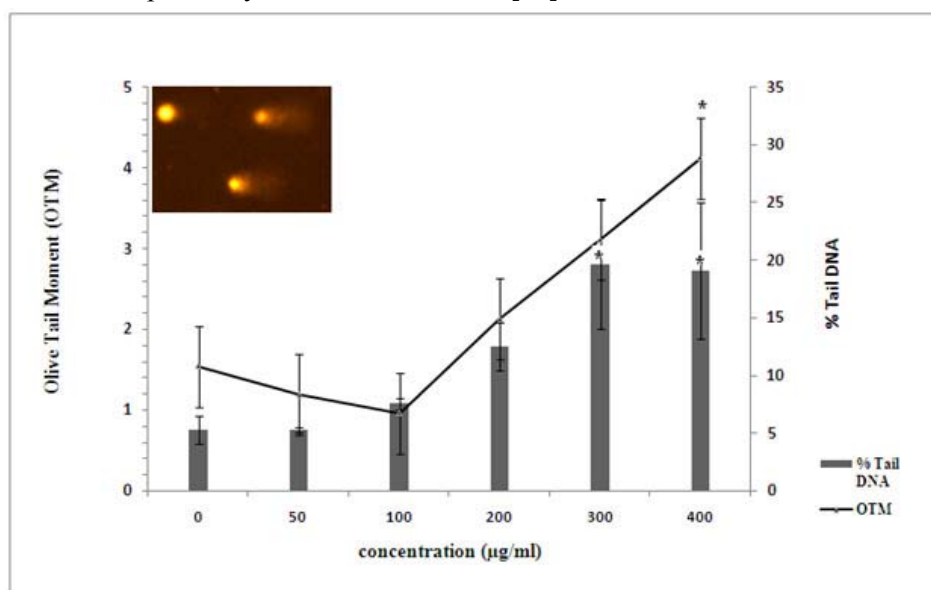


Fig. 7 Increase in DNA damage with increase in silver nanoparticles treatment concentration, represented by % Tail DNA and Olive tail moment (OTM); inset showing DNA migration as observed in comet assay. \* represents  $p < 0.050$ .

### 4. Conclusions

The growing market of silver nanoparticles, a risk of widespread exposure to man and the environment can occur [41]. It is expected that the bio kinetics of nanoparticles, which is measured as the rate of nanoparticle uptake, intracellular distribution and exocytosis, contribute tremendously to their toxicity [40]. The nanoparticle size, surface area, and surface fictionalization are major factors that influence bio kinetics and thus toxicity. Metallic silver appears to pose minimal risk to health, whereas soluble silver compounds are more readily absorbed and have the potential to produce adverse effects [42].

From the results of the above study it may be concluded that silver nanoparticles can be produced by *Alternaria alternata* mycelial biomass extracellularly. DLS, AFM and TEM analysis confirmed the uniform distribution of nanoparticles, having an average size of  $28 \pm 4.0$  nm, and its corresponding electron diffraction pattern confirmed the “fcc” (face cubic centre) crystalline structure of metallic silver. FTIR characterization confirmed the presence of protein matrix as a stabilizing agent. Based on the results on genotoxicity study, caution should be exercised on the application of silver nanoparticles on human health.

### Acknowledgements

The authors thank Dr. Aparna Laskar for carrying out TEM images and measurements using TEM facility of the Indian Institute of Chemical Biology, Kolkata, India. The authors (Krishnendu Acharya, Anita Mukherjee and Dipankar Chattopadhyay) are also grateful to Center for Research in Nanoscience and Nanotechnology, University of Calcutta for financial support.

### References

- [1] A. Krolukowska, A. Kudelski, A. Michota, J. Bukowska, Surf. Sci **532**, 227 (2003).
- [2] A. Kumar, S. Mandal, P. R. Selvakannan, R. Parischa, A. B. Mandale, M. Sastry, Lang **19**, 6277 (2003).
- [3] N. Chandrasekharan, P. V. Kamat, J. Phys. Chem. B **104**, 10851 (2000).
- [4] G. Peto, G. L. Molnar, Z. Paszti, O. Geszti, A. Beck, L. Gucci, Mater. Sci. Eng. C **19**, 95 (2002).
- [5] T. Y. Beveridge, R. G. E. Murray, J. Bacteriol **141**, 876 (1980).
- [6] N. Kuyucak, B. Volesky, Biorec **1**, 146 (1989).
- [7] N. Frilis, P. Myers-Keith, Biotechnol. Bioeng **28**, 21 (1986).
- [8] K. Acharya, J. Sarkar, S. S. Deo, Mycosynthesis of Nanoparticles in Advances in Biotechnology, Bentham Science Publishers Ltd. (2009).
- [9] A. Gade, A. Ingle, C. Whiteley, M. Rai, Biotechnol. Lett **32**, 593 (2010).
- [10] S. Saha, J. Sarkar, D. Chattopadhyay, S. Patra, A. Chakraborty, K. Acharya, Dig. J. Nanomater. Biostruc **5(4)**, 1075 (2010).
- [11] M. Sastry, A. Ahmad, I. Khan, R. Kumar, Curr. Sci **85(2)**, 162 (2003).
- [12] M. A. Hayat (ed) Colloidal Gold in Principles, methods, and applications, Academic Press, New York (1989).
- [13] S. Mann. G.A. Ozin, Natur **382**, 313 (1996).
- [14] G. Cao (ed) Nanostructures and Nanomaterials in Synthesis, Properties and Applications, Imperial College Press, London (2004).
- [15] A. Ingle, A. Gade, S. Pierrat, C. Sonnichsen, M. Rai, Curr. Nanosci **4**, 141 (2008).
- [16] D. Maity, M. K. Bain, B. Bhowmick, J. Sarkar, S. Saha, K. Acharya, M. Chakraborty, D. Chattopadhyay, J. Appl. Pol. Sci (2011) (in press)
- [17] K. Cha, H-Y. Hong, Y-G. Choi, M. J. Lee, J. H. Park, H-K. Chae, G. Ryuand, H. Myung, Biotechnol. Let **30(11)**, 1893 (2008).
- [18] S. H. Shin, M. K. Ye, H. S. Kim, Int. Immunopharmacol **74**, 1813 (2007).
- [19] V. Colvin, Natur. Biotechnol **21**, 1166 (2003).
- [20] C. K. Maiti, S. Sen, A.K. Paul, K. Acharya, J. Mycopathol. Res **45(1)**, 132 (2007).
- [21] C. V. Subramaniam, Hyphomycetes. Indian Council of Agricultural Research (ICAR). New Delhi, India (1971).
- [22] M. B. Ellis, Dematiaceous Hyphomycetes. Commonwealth Mycological Institute (CMI), Kew, UK (1971).
- [23] M. B. Ellis, More Dematiaceous Hyphomycetes. Commonwealth Mycological Institute (CMI), Kew, UK (1976).
- [24] A. Boyum, Scand. J. Immunol. Suppl **5**, 9 (1976).
- [25] J. R. Tennant, Transplant **2**, 685 (1964).

- [26] L. Henderson, E. Jones, T. Brooks, A. Chetelat, P. Ciliutti, M. Freemantle, C. A. Howard, J. Mackay, B. Phillips, S. Riley, C. Roberts, A. K. Wotton, E. J. van de Waart, *Mutag* **12**, 163 (1997).
- [27] N. P. Singh, M. T. McCoy, R. R. Tice, E. L. Schneider, *Exp. Cell. Res* **175**, 184 (1988).
- [28] A. Bandyopadhyay, S. Ghoshal, A. Mukherjee, *Drug. Chem. Toxicol* **31**, 447 (2008).
- [29] R. R. Tice, E. Agurell, D. Anderson, B. Burlinson, A. Hartmann, H. Kobayashi, *Environ. Mol. Mutag* **35**, 206 (2000).
- [30] A. Henglein, *J. Phys. Chem* **97(21)**, 5457 (1993).
- [31] Z. Lin, J. Wu, R. Xue, Y. Yong, *Spectrochim. Acta. Part. A* **61**, 761 (2005).
- [32] A. Tripathy, A. M. Raichur, N. Chandrasekaran, T. C. Prathna, A. Mukherjee, *J. Nanopart. Res* **12**, 237 (2010).
- [33] N. Vigneshwaran, A. A. Kathe, P. V. Varadarajan, R. P. Nachane, R. H. Balasubramanya, *Lang* **23**, 7113 (2007).
- [34] L. Jin, R. Bai, *Lang* **18**, 9765 (2002).
- [35] S. Shankar, A. Ahmad, M. Sastry, *Biotechnol. Prog* **19**, 1627 (2003).
- [36] L. Luo, S. Yu, S. Quin, T. Zhou, *J. Am. Chem. Soc* **127**, 2822 (2005).
- [37] J. Huang, Q. Li, D. Sun, Y. Lu, Y. Su, X. Yang, *Nanotechnol* **18**, 105104 (2007).
- [38] R. Sanghi, P. Verma, *Biores. Tech* **100**, 501 (2009).
- [39] H. W. Lu, S. H. Liu, X. L. Wang, X. F. Qian, J. Yin, J. K. Jhu, *Mater. Chem. Phys* **81**, 104 (2003).
- [40] P. V. AshaRani, G. L. K. Mun, M. P. Hande, S. Valiyaveetil, *ACS Nano* **2**, 279 (2009).
- [41] S. W. P. Wijnhoven, W. J. G. M. Peijnenburg, C. A. Herberts, W. I. Hagens, A. G. Oomen, E. H. W. Heugens, B. Roszek, J. Bisschops, I. Gosens, D.V. D. Meent, S. Dekkers, W. H. D. Jong, M. V. Zijverden, A. J. A. M. Sips, R. E. Geertsma, *Nanotoxicol* **3(2)**, 109 (2009).
- [42] P. L. Drake, K. J. Hazelwood, *Ann. Occup. Hyg* **49**, 5